Supporting Information

Insights into the Importance of DFD-Motif and Insertion I1 in Stabilizing the DFD-Out Conformation of Mnk2 Kinase

Jinqiang Hou, Theodosia Teo, Matthew J. Sykes, and Shudong Wang*

Centre for Drug Discovery and Development, Sansom Institute for Health Research and School of Pharmacy and Medical Sciences, University of South Australia, Adelaide SA 5001, Australia

*Corresponding author: Email: shudong.wang@unisa.edu.au Tel.: +61-8-8302-2372

Content

S1. Methodology for homology modelling

S2. Methodology for the high temperature molecular dynamics simulation

Table S1. Top 10 identified structural analogues in the PDB

Table S2. Mnk2 and Mnk2-mutant models for the MD simulations

Figure S1. The rmsf plots of the residues of Mnk2 and Mnk2-mutant models

Figure S2. The distance of phenyl rings between Phe159 (gatekeeper) and Phe227 in Mnk2-in model at a temperature of 300 K.

Figure S3. The time-evolution of the DFD-motif with reference to the homology models built for the repeated stimulation studies.

Figure S4. The time course of rmsd values of the A-loop backbone atoms with respect to the corresponding starting structures of the homology models.

Figure S5. Superimposition of starting structures and averaged structures calculated from the last 4 ns trajectories.

Figure S6. Simulation structures from the Mnk2-out model.

Figure S7. Superimposition of initial structure and the averaged structure taken from the last 4 ns trajectory of Mnk2DFG-in or Mnk2-DFG-out models.

Figure S8. Superimposition of the initial structure and averaged structure taken from the last 4 ns trajectory of Mnk2mutant-in or Mnk2mutant-out models.

Figure S9. Superimposition of the initial structure and averaged structure taken from the last 4 ns trajectory of Mutant-in or Mutant-out models.

Figure S10. Snapshots of the simulation models elucidating the conformational change of the activation loop.

Movies The movies show the flips from –in to –out in the model of Mnk2-in and from – out to –in in the model of Mutant-out.

References.

S1. Methodology for homology modeling

The Mnk2-kinase domain (Mnk2-KD) is activated by phosphorylation via upstream kinases such as extracellular-signal-regulated kinase (ERK) and p38 kinase in the C-terminus A-loop, thus restoring the function of the full-length protein.[1] The crystal structures of Mnk2 solved by Jauch *et al.* showed a missing portion encompasses part of the activation loop (residues 232-250),[2] including the two phosphorylation sites (i.e. Thr244 and Thr249) for upstream activating kinases.[2] Another region corresponds to part of the so-called insertion I3 with specific cysteine clusters (residues 304-310; tip of the zinc finger)[2] and is partially missing due to the lack of interpretable electron density.[2] Initially, the Mnk2-KD homology model was generated by exploiting a resolved crystal structure (PDB entry 2AC3) as template, followed by multiple threading alignments, as implemented in the I-TASSER approach (http://zhanglab.ccmb.med.umich.edu/I-TASSER/).[3,4] The online I-TASSER server automatically aligns the target sequence with potential hits found in the PDB library, and sends the best-matched results, up to 10 predicted models, back to the user. Information detailing TM-score, rmsd, percentage sequence identity and the coverage of the alignment are also provided as presented in Table S1. Other mutant models, including a single mutation of D228 to G228, as well as the removal of insertion I (Table S2) were then built by Modeller version 9.11,[5] using the initial homology model as template. A preliminary energy minimization was performed on the activation loop to avoid high-energy interactions. It was essential to retain the Zn^{2+} ion in all models as this ion is coordinated by four conserved cysteine residues in the Mnk2-KD, forming an extensive zinc finger-like network.[2]

S2. Methodology for the high temperature molecular dynamics simulation

The developed 3D homology model of the Mnk2-KD was further refined via MD simulations. All MD simulations were carried out with the Molecular Dynamics (MD) module of the Amber12 suite[6] using the AMBER ff10 force field,[7] with the exception of the zinc ion. The force field for Zn^{2+} required special parameters that can be found in the cationic dummy atom (CaDA) approach (http://mayoresearch.mayo.edu/mayo/research/camdl/zinc_protein.cfm). Every protein model was immersed in a truncated octahedral box of TIP3P water molecules, extending up to 10 Å from the solute in each direction. Sodium counter-ions were subsequently added to the system for charge neutralization on the protein backbone. By using the Coulombic potential, these counter-ions were assigned automatically to the most negative locations with the LEAP program.[6]

All protein models were subjected to initial minimization to equilibrate the solvent and counter-ions. The proteins were initially fixed with a force constant of 50 kcal mol^{-1} $Å^{-1}$. A 2,000-step full minimization was carried out throughout the system without applying restraints. The systems were then slowly heated from 0 to 1000 K over 1 ns at constant volume with a force constant of 50 kcal mol^{-1} $Å^{-1}$ to prevent protein unfolding. After the heating process, a further 500 ps of equilibration using a 10 kcal mol^{-1} $Å^{-1}$ constraint on the entire protein was carried out to obtain a stable density. Then the restraints were removed in the A-loop (residues 224-260) to allow complete free motion of the loop, while keeping a constraint of 10 kcal mol^{-1} $Å^{-1}$ on the rest of the protein. The run was continued at 1000 K for a further 50 ns simulation. All MD simulations were carried out in a canonical (NVT) ensemble, where the number of particles, volume and temperature of the system were kept constant. A residue-based cut-off of 10 Å was used for the non-bonded interactions. The hydrogen bonds were constrained using the SHAKE algorithm.[8] Periodic boundary

conditions were applied throughout the system to avoid the edge effect. The Particle Mesh Ewald (PME) method was employed to calculate long-range electrostatic interactions.[9] Temperature regulation was achieved by the Berendsen Thermostat. The time step used for the MD simulations was set to 2.0 fs, and the trajectory files were collected every 100 ps for the subsequent analysis. All trajectory analyses were implemented with the PTRAJ module in the Amber12 suite and were examined visually using VMD software.[10]

Table S1. Top 10 identified structural analogues in the PDB

Rank	PDB Hit	TM-score	RMSD[a]	IDEN[b]	Cov.[c]
1	3mfsA	0.891	1.62	0.356	0.944
2	2y7jA	0.882	2.03	0.348	0.955
3	1ql6A	0.880	1.94	0.341	0.952
4	1jksA	0.873	1.93	0.352	0.944
5	2yabA	0.873	1.93	0.356	0.944
6	2vn9B	0.869	1.77	0.352	0.933
7	2v7oA	0.867	2.02	0.340	0.944
8	2vz6B	0.867	1.87	0.359	0.937
9	3q5iA	0.866	1.68	0.372	0.922
10	3lijA	0.860	1.79	0.411	0.918

Ranking of proteins is based on TM-score of the structural alignment between the query structure and known structures in the PDB library. RMSD[a] is the rmsd between residues that are structurally aligned by TM-align. IDEN[b] is the percentage sequence identity in the structurally aligned region. Cov.[c] represents the coverage of the alignment by TM-align and is equal to the number of structurally aligned residues divided by length of the query protein.

Table S2. Mnk2 and Mnk2-mutant models for the MD simulations

Models	Mutation	Simulation time (ns)	Temperature (K)	Repeat
Mnk2-in	Non-mutant homology model	200	300	1
Mnk2-in	Non-mutant homology model	80	1000	2
Mnk2-out	Non-mutant homology model	50	1000	2
Mnk2mutant-in	Insertion I1 removed	50	1000	2
Mnk2mutant-out	Insertion I1 removed	50	1000	2
Mnk2DFG-in	DFG replaced with DFD	50	1000	2
Mnk2DFG-out	DFG replaced with DFD	50	1000	2
Mutant-in	Insertion I1 removed and DFG replaced with DFD	50	1000	2
Mutant-out	Insertion I1 removed and DFG replaced with DFD	50	1000	2

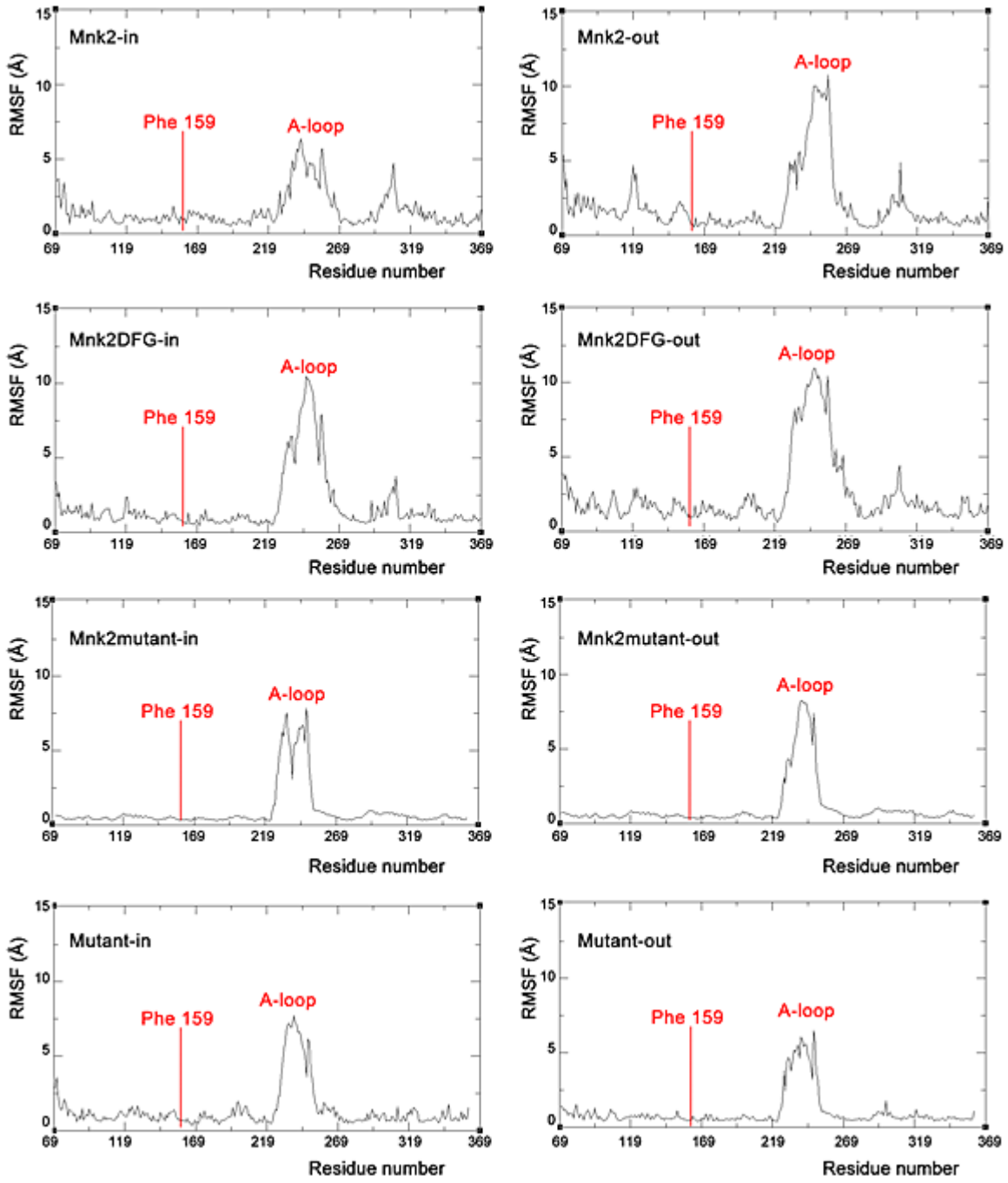

Figure S1. The rmsf plots of the residues of Mnk2 and Mnk2-mutant models. Mass-weighted RMSF values for each residue from entire simulation trajectories were analysed using the PTRAJ module in the AMBER suite. The non A-loop residues are stable with a 10 kcal mol^{-1} $Å^{-1}$ constraint.

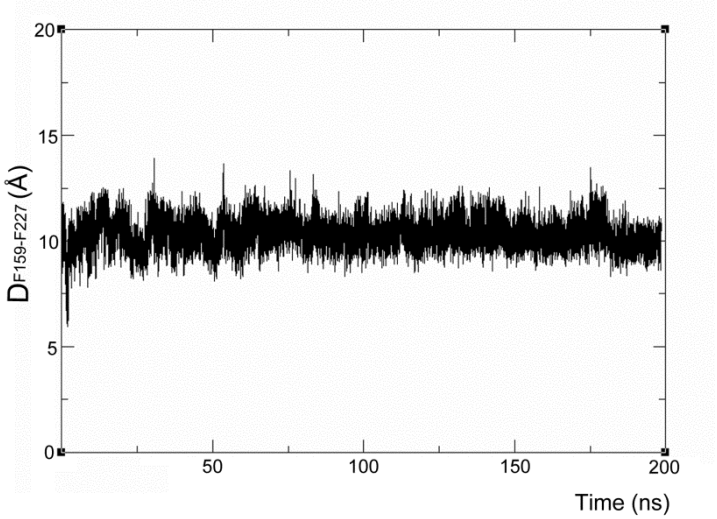

Figure S2. The distance of phenyl rings between Phe159 (gatekeeper) and Phe227 in model Mnk2-in at a temperature of 300 K. No appreciable conformational change of the DFD-motif was observed in a 200 ns simulation, indicating that the time scale for DFD-flip is much longer than a few hundred nanoseconds.

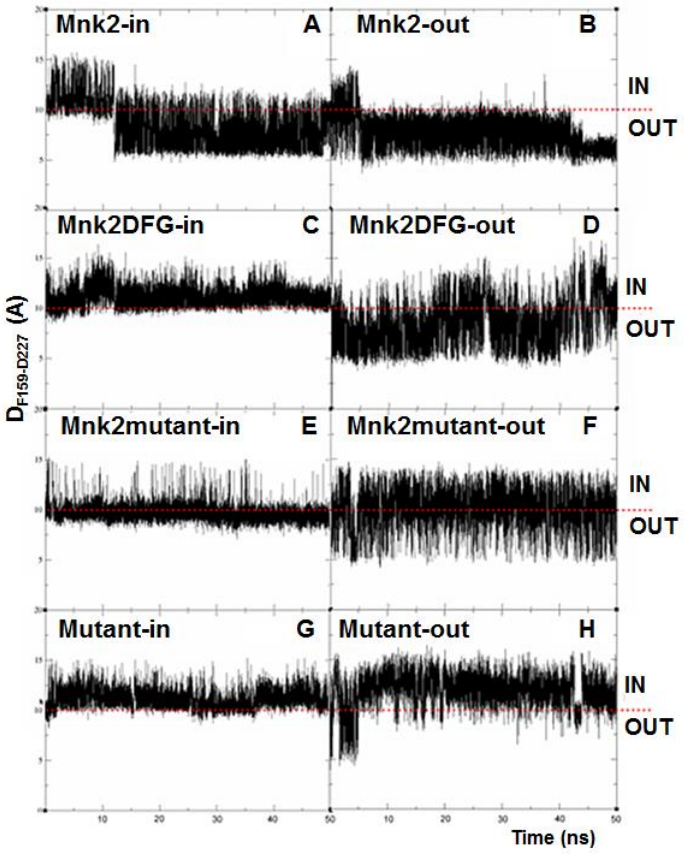

Figure S3. (A-H) The time-evolution of the DFD-motif with reference to the homology models built for the repeated stimulation studies. The $D_{F159\text{-}F227}$ versus simulation time (ns) plots were prepared and analyzed using the PTRAJ module in the AMBER suite while trajectories were visualized and validated using VMD software. As suggested by visual inspection of trajectories, when $D_{F159\text{-}F227}$ = 5-10 Å, the DFG/D-out conformation was adopted; when $D_{F159\text{-}F227}$ = 10-15 Å, the DFG/D-in conformation was adopted; when $D_{F159\text{-}F227}$ = 5-15 Å, all the DFG/D conformations were sampled.

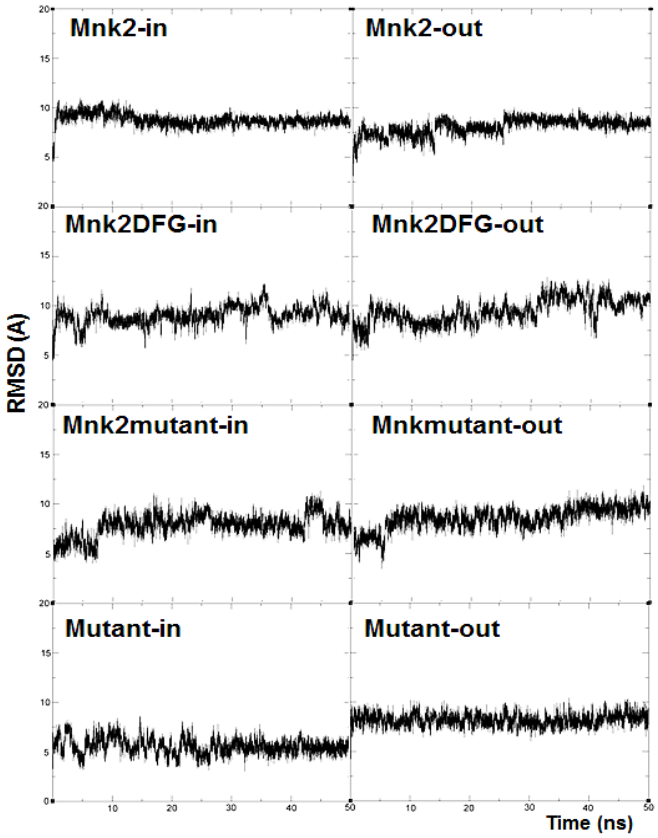

Figure S4. The time course of rmsd values of the A-loop backbone atoms (*N*,*CA*,*C*) with respect to the corresponding starting structures of the homology models. Except for the Mutant-in model, the rmsd values for all models oscillate to ~10 Å within the first few ns of MD-equilibration and reach a plateau for the rest of simulation. The rmsd for the Mutant-in model assumes lower values oscillating around 5 Å, suggesting that the A-loop is highly stable and does not move significantly away from its initial active-like conformation.

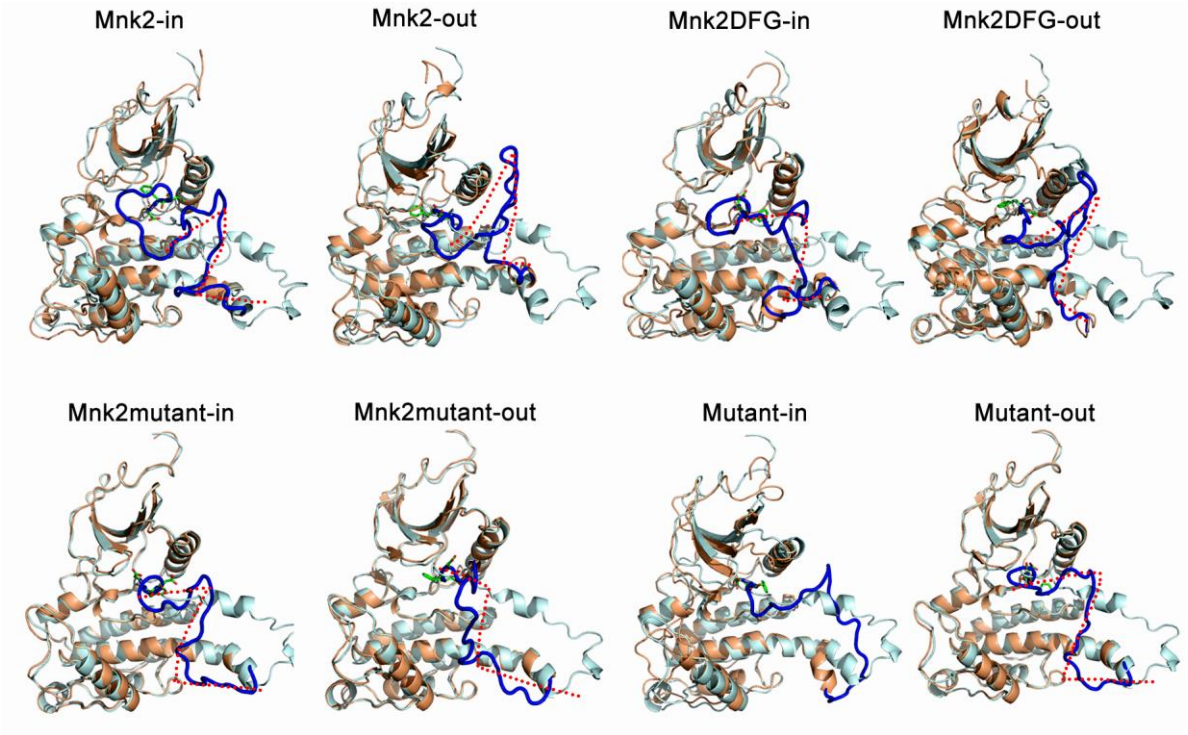

Figure S5. Superimposition of starting structures (cyan) and averaged structures calculated from the last 4 ns trajectories (bronze). The DFD-motif and the A-loop in the averaged structures are shown in green sticks and blue cartoons, respectively. The A-loop in the Mutant-in model stays in an open-like conformation, while the A-loop in the other models reaches a helical intermediate state, as indicated by the red dotted line.

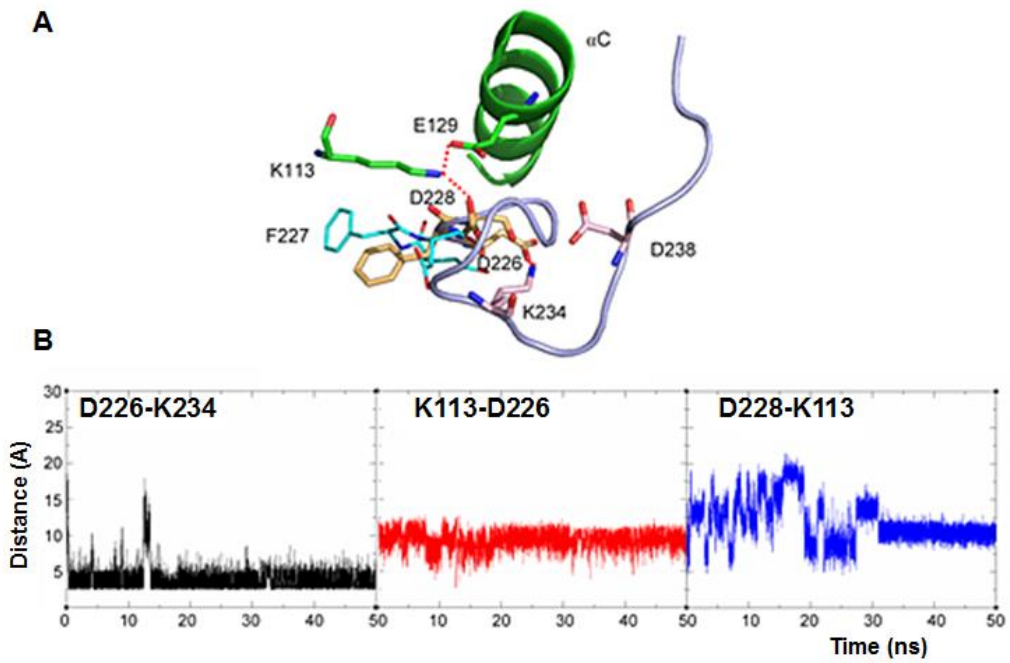

Figure S6. Simulation structures and data from the Mnk2-out model. (A) Superimposition of the initial structure (cyan sticks) and the averaged structure taken from the last 4 ns trajectory; (B) Interatomic distances for key salt-bridge interactions. The DFD-motif is shown in yellow sticks: insertion I1 is shown in pink sticks; salt-bridge interactions are shown by red dotted lines.

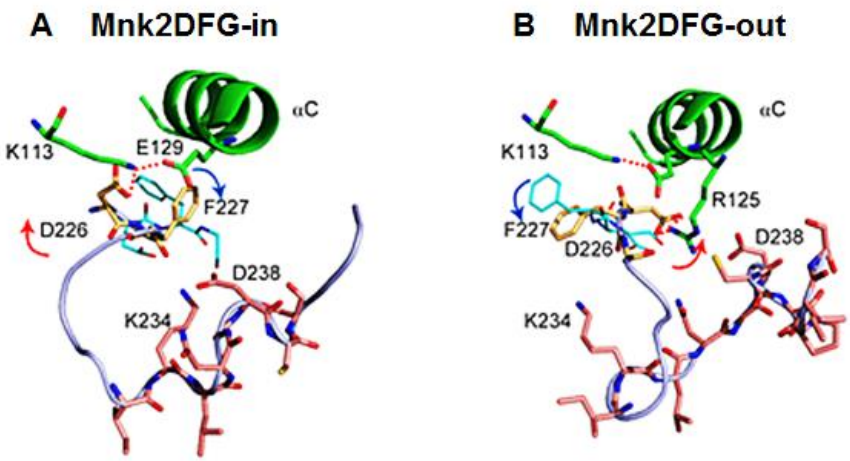

Figure S7. Superimposition of initial structure (cyan sticks) and averaged structure taken from the last 4 ns trajectory of (A): Mnk2DFG-in and (B): Mnk2DFG-out models. The DFD-motif is shown in yellow sticks; insertion I1 is shown in pink sticks; salt-bridge interactions are shown by red dotted lines. The rotation motion of D226 and F227 are shown in red and blue arrows, respectively.

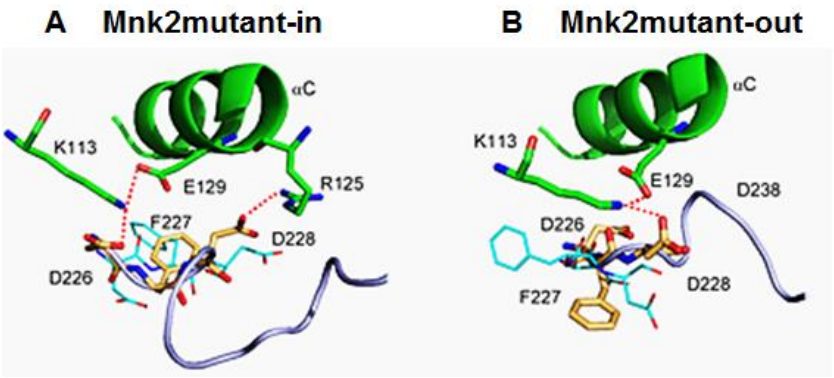

Figure S8. Superimposition of the initial structure (cyan sticks) and averaged structure taken from the last 4 ns trajectory of (A) Mnk2mutant-in and (B) Mnk2mutant-out models. The DFD-motif is shown in yellow sticks; salt-bridge interactions are shown by red dotted lines.

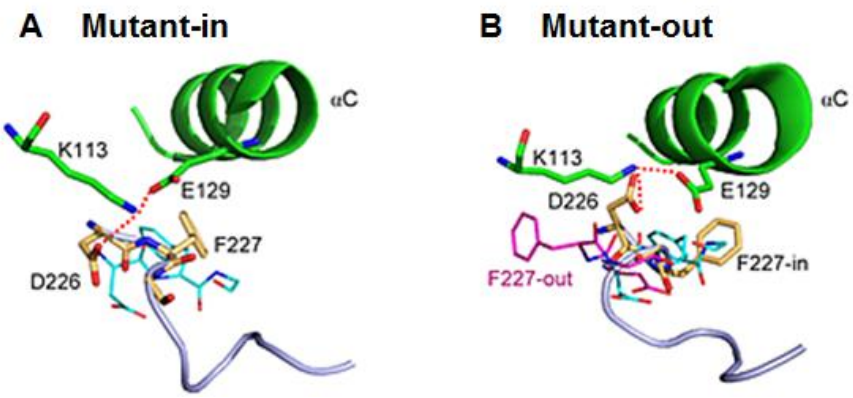

Figure S9. Superimposition of the initial structure (cyan sticks: DFD-in; pink sticks: DFD-out) and averaged structure taken from the last 4 ns trajectory of (A) Mutant-in and (B) Mutant-out models. The DFD-motif is shown in yellow sticks; salt-bridge interactions are shown by red dotted lines.

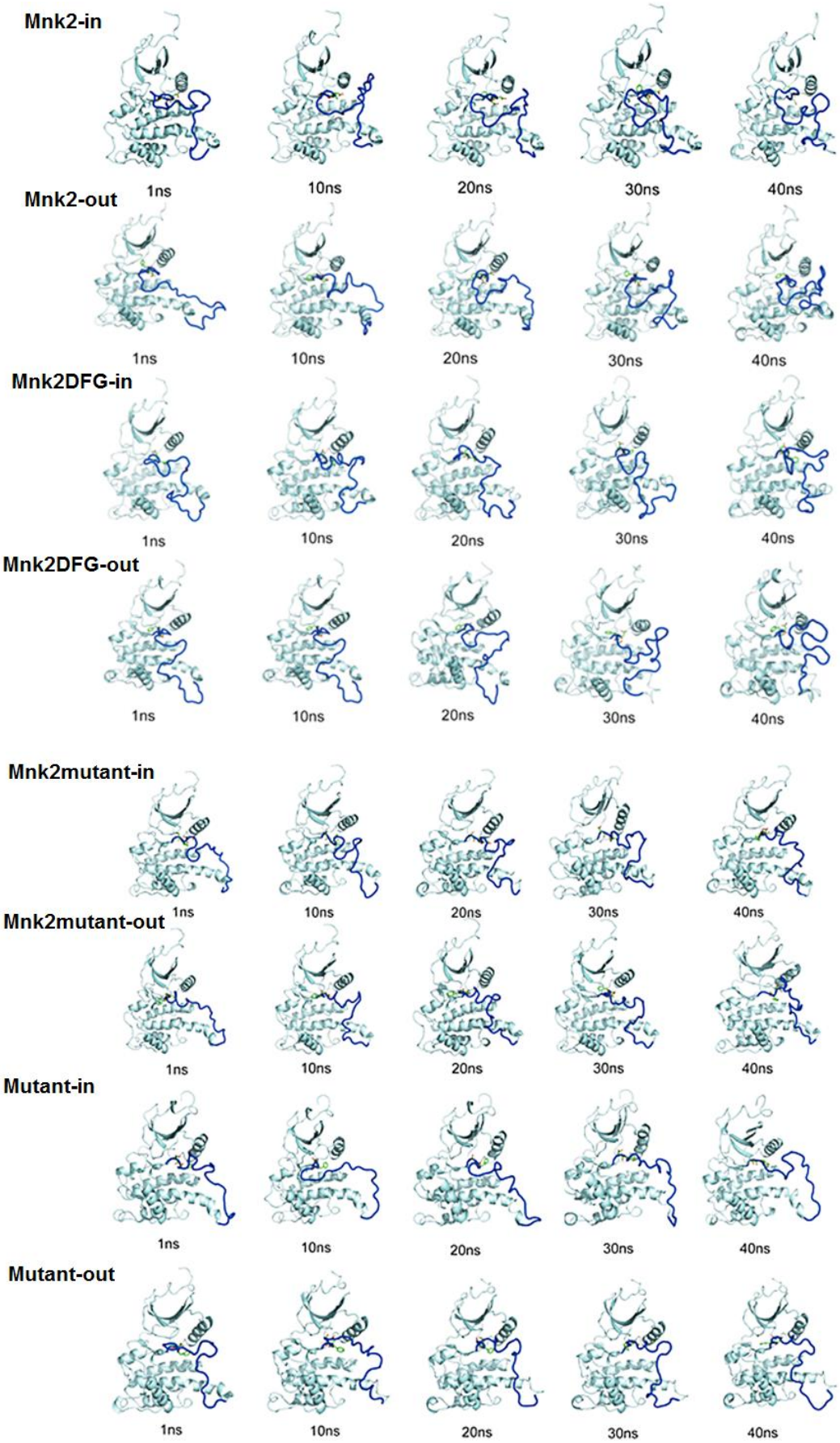
Mnk2-in
1ns
10ns
20ns
30ns
40ns
Mnk2-out
1ns
10ns
20ns
30ns
40ns
Mnk2DFG-in
1ns
10ns
20ns
30ns
40ns
Mnk2DFG-out
1ns
10ns
20ns
30ns
40ns
Mnk2mutant-in
1ns
10ns
20ns
30ns
40ns
Mnk2mutant-out
1ns
10ns
20ns
30ns
40ns
Mutant-in
1ns
10ns
20ns
30ns
40ns
Mutant-out
1ns
10ns
20ns
30ns
40ns

Figure S10. Snapshots of the simulation models elucidating the conformational change of the activation loop. The DFD-motif and the activation loop are shown in green stick and blue cartoons, respectively.

References

(1) Waskiewicz, A. J.; Flynn, A.; Proud, C. G.; Cooper, J. A. Mitogen-activated protein kinases activate the serine/threonine kinases Mnk1 and Mnk2. *EMBO J* **1997**, *16*, 1909-1920.

(2) Jauch, R.; Jakel, S.; Netter, C.; Schreiter, K.; Aicher, B.; Jackle, H.; Wahl, M. C. Crystal structures of the Mnk2 kinase domain reveal an inhibitory conformation and a zinc binding site. *Structure* **2005**, *13*, 1559-1568.

(3) Zhang, Y. I-TASSER server for protein 3D structure prediction. *BMC Bioinformatics* **2008**, *9*, 40.

(4) Roy, A.; Kucukural, A.; Zhang, Y. I-TASSER: a unified platform for automated protein structure and function prediction. Nat Protoc 2010, 5, 725-738.

(5) Eswar, N.; Webb, B.; Marti-Renom, M. A.; Madhusudhan, M. S.; Eramian, D.; Shen, M. Y.; Pieper, U.; Sali, A. Comparative protein structure modeling using MODELLER. *Curr Protoc Protein Sci* **2007**, *Chapter 2*, Unit 2 9.

(6) Case, D. A.; Darden, T. A.; Cheatham, I., T.E.; Simmerling, C. L.; Wang, J.; Duke, R. E.; Luo, R.; Walker, R. C.; Zhang, W.; Merz, K. M.; Roberts, B.; Hayik, S.; Roitberg, A.; Seabra, G.; Swails, J.; Goetz, A. W.; Kolossváry, I.; Wong, K. F.; Paesani, F.; Vanicek, J.; Wolf, R. M.; Liu, J.; Wu, X.; Brozell, S. R.; Steinbrecher, T.; Gohlke, H.; Cai, Q.; Ye, X.; Wang, J.; Hsieh, M.-J.; Cui, G.; Roe, D. R.; Mathews, D. H.; Seetin, M. G.; Salomon-Ferrer, R.; Sagui, C.; Babin, V.; Luchko, T.; Gusarov, S.; Kovalenko, A.; Kollman, P. A. AMBER 12. **2012**, *University of California, San Francisco.*

(7) Cornell, W. D.; Cieplak, P.; Bayly, C. I.; Gould, I. R.; Merz, K. M.; Ferguson, D. M.; Spellmeyer, D. C.; Fox, T.; Caldwell, J. W.; Kollman, P. A. A Second Generation Force Field for the Simulation of Proteins, Nucleic Acids, and Organic Molecules. *J Am Chem Soc* **1995**, *117*, 5179-5197.

(8) Ryckaert, J.-P.; Ciccotti, G.; Berendsen, H. J. C. Numerical integration of the cartesian equations of motion of a system with constraints: molecular dynamics of n-alkanes. *J Comput Phys* **1977**, *23*, 327-341.

(9) Darden, T.; York, D.; Pedersen, L. Particle mesh Ewald: An N·log(N) method for Ewald sums in large systems. J Chem Phys **1993**, *98*, 10089-10092.

(10) Humphrey, W.; Dalke, A.; Schulten, K. VMD: Visual molecular dynamics. J Mol Graph **1996**, *14*, 33-38.